LACBED Characterisation of Dislocation Loops

Jean-Paul Morniroli, Ross Marceau, Simon Ringer, Loïc Boulanger

LACBED Characterisation of Dislocation Loops

Journal:	*Philosophical Magazine & Philosophical Magazine Letters*
Manuscript ID:	TPHM-05-Dec-0551.R2
Journal Selection:	Philosophical Magazine
Date Submitted by the Author:	10-Mar-2006
Complete List of Authors:	MORNIROLI, Jean-Paul; Laboratoire de Métallurgie et Génie des Matériaux, UMR CNRS 8517, USTL & ENSCL Marceau, Ross; Australian Key Centre for Microscopy & Microanalysis, The University of Sydney Ringer, Simon; Australian Key Centre for Microscopy & Microanalysis, The University of Sydney Boulanger, Loïc; Service de Recherche de Métallurgie Physique, CEA/Saclay
Keywords:	crystal defects, dislocations, electron diffraction
Keywords (user supplied):	

LACBED Characterisation of ~~Small~~ Dislocation Loops

J.P. MORNIROLI[*1], R.K.W. MARCEAU[2], S.P. RINGER[2] and L. BOULANGER[3]

[1] Laboratoire de Métallurgie Physique et Génie des Matériaux, UMR CNRS 8517, USTL & ENSCL, Cité Scientifique, 59500 Villeneuve d'Ascq, France

[2] Australian Key Centre for Microscopy & Microanalysis, the University of Sydney NSW, 2006 Australia

[3] Service de Recherche de Métallurgie Physique, CEA/SACLAY, 91191 Gif Sur Yvette, France

Corresponding author : J.P. Morniroli, Laboratoire de Métallurgie Physique et Génie des Matériaux, UMR CNRS 8517, USTL & ENSCL, Bâtiment C6, Cité Scientifique, 59500 Villeneuve d'Ascq, France

Email: Jean-Paul.Morniroli@univ-lille1.fr

Abstract

The characterisation of the amplitude and sign of the Burgers vector of perfect or partial dislocations from Large-Angle Convergent-Beam Electron Diffraction (LACBED) patterns is now a routine technique following the original idea proposed by Cherns and Preston. The technique has already been applied to large dislocation loops present in semiconductors but in many specimens submitted to irradiation, implantation or thermal treatments, the size of the dislocation loops that are encountered are too small to be identified from normal LACBED experimental conditions. The aim of this paper is to propose solutions to enable the analysis

of small dislocation loops, with diameter less than 100 nm. Examples of perfect and partial dislocation loops present in austenitic steels, Al-Cu-Mg alloys and in doped silicon are given in which the vacancy or the interstitial type of the loops is inferred. The minimum loop size that can be studied with the present technique is about 30 nm. The present technique is similar in its capabilities to the range of methods based on the "inside-outside" contrast observed on weak-beam images but is has some main operational advantages: the experiments are easy to perform and to interpret and no specific crystal orientation is required.

Keywords: Electron diffraction, dislocations, dislocation loops

Introduction

Dislocation loops are frequently observed in specimens submitted to irradiation, implantation or thermal treatments. The characterisation of these loops, especially the identification of the vacancy or the interstitial type, is important since it is strongly connected with the physical or mechanical properties. Conventional methods to deduce the Burger vector involve Transmission Electron Microscopy (TEM) micrographs and are based on the invisibility criterion. The loop plane is obtained from trace analysis and the vacancy or interstitial type is obtained from observation of specific contrasts that occur on two-beam electron micrographs. For small loops down to a size about 10 nm, the conventional "inside outside" method with weak beam imaging can be used to determine the loop nature. Other methods were developed for loops smaller than 10 nm in size [1, 2]. Nevertheless, the corresponding experiments are not easy to perform especially in the case of very small loops.

In 1986, Cherns and Preston [3] demonstrated the possibility of using the "splittings", which occur at the intersection of the Bragg lines within LACBED patterns with the shadow image of the dislocation lines, to deduce both the amplitude and the sign of the Burgers vectors. In addition to this, LACBED patterns can also be used to characterise the line direction **u** [4]. The technique was successfully applied to perfect and partial dislocations present in various materials [5, 6], and is especially useful in the case of anisotropic and beam-sensitive materials [7, 8].

Application of this LACBED technique to large dislocation loops that are present in semiconductors has been made by Tanaka et al. [5] and Jäger et al. [9] but in the case of dislocation loops with size smaller than 100 nm, it is usually unsuccessful since two main difficulties are observed under normal LACBED experimental conditions.

The first difficulty is concerned with the size of the shadow image of the dislocation loop with respect to the diffraction pattern. It is usually too small so that the splittings required for analysis are poor or not visible.

The second difficulty is concerned with the contrast of the dislocation loop, which is strongly dependent on the diffraction conditions. When the shadow image of the dislocation line is moved from one Bragg line to another in order to obtain a new splitting, its contrast can change drastically and eventually disappear. In this case, it becomes very difficult to avoid confusing the loop that is being studied with other loops located within the vicinity.

The aim of this paper is to describe experimental methods to solve these two problems and to allow fast, unambiguous characterisation of small dislocation loops.

Description of the LACBED technique

The LACBED technique was proposed by Tanaka et al. [10] to overcome the problem of the superimposition of the excess and deficiency lines present in Convergent-Beam Electron Diffraction (CBED) patterns, which occurs when the convergence angle of the incident beam becomes larger than the Bragg angle. In this technique, a large-angle incident beam (in the range 1 to 5°) is focused on the object plane of the objective lens of a transmission electron microscope (Figure 1). The specimen is not located in this object plane, as it is usually, but rather above (defocus value $\Delta h > 0$) or below (defocus value $\Delta h < 0$) it. For a set of (hkl) lattice planes, the hkl and -h-k-l diffraction phenomena occur along the two parallel lines AB and CD of the specimen, giving rise to hkl and -h-k-l diffracted beams that separate from the transmitted beam in the object plane (points E, K and L) and in its conjugate image plane (points E', K' and L') where the transmitted beam is selected by means of the selected-area aperture. For the sake of clarity, this aperture is drawn in Figure 1 on the object plane where it has the same effect. The Bright-Field (the transmitted disk) pattern is observed in the back

focal plane of the objective lens and contains two parallel hkl and -h-k-l deficiency lines (called Bragg lines). The corresponding deviation parameter s equals 0 on each Bragg line and varies positively and negatively along parallel lines as shown on Figure 1b.

In fact, many sets of (hkl) lattice planes (the planes which are parallel or nearly parallel to the optical axis of the microscope) are simultaneously in diffraction condition so that the resulting LACBED pattern usually contains many Bragg lines. It is pointed out that the diffraction pattern does not depend on the Δh value.

The LACBED patterns display three interesting properties.

- Since it is a defocus technique, the image of the illuminated area of the specimen is also visible in the back focal plane of the objective lens. This image is not exactly in focus and for this reason it is called a "shadow" image. Its magnification depends on the Δh value. Taking into account this property, a LACBED pattern can be considered as an image-diffraction mapping displaying simultaneously information about the direct space (the shadow image) and the reciprocal space (the Bragg lines).

- LACBED patterns display an excellent quality with respect to the corresponding CBED patterns. This property is due to the selected-area aperture, which acts as an efficient angular filter and removes most of the inelastically scattered electrons [11].

- The dose received by the specimen is low since the incident beam is defocused. This means that the LACBED technique can be used with beam-sensitive materials and that contamination of the specimen remains insignificant.

LACBED pattern in the presence of a dislocation

As mentioned above, a LACBED pattern is an image-diffraction mapping and the displacement field located around a dislocation line can distort this mapping. Cherns and

Preston identified typical effects that occur at the intersection of Bragg lines with the shadow image of a dislocation line, and these can be used to identify the Burgers vector.

These typical effects, called "splittings" in the present context, consist of a local rotation of the Bragg line associated with a separation of the line into interfringes. From simulated patterns, Cherns and Preston indicated that the number of interfringes, n, is directly connected with the **g.b** dot product where $\mathbf{g}=h\mathbf{a}_1^*+k\mathbf{a}_2^*+l\mathbf{a}_3^*$ is the reciprocal lattice perpendicular to the (hkl) lattice planes and $\mathbf{b}=u\mathbf{a}_1+v\mathbf{a}_2+w\mathbf{a}_3$, the Burgers vector. If the sign of deviation parameter, s, is also taken into account, then the sign of n can be obtained from the Cherns and Preston rules given in Figure 2.

In order to identify the Burgers vector from the LACBED splittings, two procedures may be considered:

If the Burgers vector is unknown, at least three splittings must be observed in order to establish the following system of three linear equations:

$\mathbf{g}_1.\mathbf{b}=n_1$

$\mathbf{g}_2.\mathbf{b}=n_2$

$\mathbf{g}_3.\mathbf{b}=n_3$

The three components [uvw] of the Burgers vector are obtained by solving this set of equations. To obtain the required splittings, the dislocation line is moved from one Bragg line to another by shifting or tilting the specimen. To avoid indeterminacy, the three Bragg lines involved must not come from the same [uvw] zone axis.

If the form, but not the exact indices of the Burger vector is known (for example, a ½<110> form), then it is better to compare several experimental n values with a table giving the n values calculated for all the possible vectors (for example, for the 12 vectors belonging to the ½<110> form). This solution is particularly useful when partial dislocations are considered because the n values are not always integer in this case.

Best experimental conditions

For a tilted dislocation line present in a specimen (Figure 3), good splittings are obtained when the following experimental conditions are fulfilled:

- The best splittings are observed for the part of the dislocation line located in the middle of the thin foil (Figure 3a). Experimentally, this means that the shadow image of a dislocation line should be carefully positioned with respect to a Bragg line.

- The diffraction pattern and therefore the deviation parameter, s, of a Bragg line do not depend on the defocus value Δh. This is not the case for the shadow image of the displacement field located around the dislocation line whose magnification depends on Δh (Figure 3b). As a result, the splitting aspect changes with Δh as shown schematically on Figure 3b. The defocus value Δh should be selected so that the splittings are clearly visible and so that their interfringe number n can be counted without ambiguity.

Depending on the positive or negative sign of the defocus value Δh, the shadow image of a dislocation line is either rotated an angle of 180° with respect to its direction in the specimen or not rotated at all (Figure 3c). For Burgers vector identification, this means that all the splittings must be obtained with the same sign for Δh.

- The best splittings are observed when the Bragg line and the shadow image of the dislocation line are perpendicular or nearly perpendicular. If not, the splittings become distorted (Figure 3d). Nevertheless, this condition is not very strict and very large misorientations can be used provided the n value can still be identified.

Two types of Bragg lines are observed on LACBED patterns. Reflections with an extinction distance smaller than about 100 nm display strong intensity and dynamical behaviour giving Bragg lines that are made up of a set of fringes (see, for example, Figure 6). These Bragg lines

display complex splittings at the intersection with a dislocation line and are not well suited for Burgers vector identification.

Reflections having a larger extinction distance have quasi-kinematical or kinematical behaviour and the resulting Bragg line only displays a unique intensity minimum at the exact Bragg orientation (at s=0). Provided, they are not to weak, these reflections are better suited and must be selected for the present analysis.

The choice of n is also important. If n is too large, then it becomes difficult to count the number of interfringes.

The thickness of the specimen plays also an important role. If the specimen is too thin, the Bragg lines are broadened and the splittings display poor quality. In addition, thin areas are often buckled and give distorted LACBED patterns. Under normal conditions, ideal specimen thickness is in the range 50 to 400 nm for most specimens.

Particular case of partial dislocations

With perfect dislocations, the dot product **g.b** has always an integer value. This is not the case with partial dislocations, which are located at the edges of stacking faults and have corresponding **g.b** values that are non-integral. For example, with Frank partial dislocations present in FCC structures, the values 1/3, 2/3, 1, 4/3, 5/3, 2, 7/3…. are encountered. From simulated patterns, Tanaka et al. [5] indicated that the actual n value can be obtained provided the fine structure and the intensity of the splittings are taken into account. Another solution used by Morniroli et al [12] consists of observing specific Bragg lines that are not affected by the stacking fault connected with the studied partial dislocation. In this case, the **g.b** value is integral. Stair rod partial dislocations located at the edges of stacking fault pyramids were characterised in that way.

Conventions

The analysis of the sign of the Burgers vector requires some conventions. In the present study, we used the following conventions:

- The thin foil normal, $\mathbf{B}=[u_B v_B w_B]$, and loop normal, $\mathbf{N_{Loop}}$, are directed upwards (in the opposite direction to the incident beam).

- The FS/RH convention in the perfect crystal is used to describe the Burgers vector (Figure 4d).

- For a dislocation line, the direction of the line, **u**, is chosen arbitrarily. For a dislocation loop, the line direction, **u**, as seen on the electron micrographs and on the LACBED patterns, is chosen according to the anticlockwise direction (Figure 4a).

With these conventions, vacancy and interstitial loops are shown schematically in Figures 4b and 4c respectively. Other loops having a more or less appreciable shear character may also be encountered. They are not described here since they were not observed in the present study.

Specific problems connected with small dislocation loops

Two specific and major problems are encountered with small loops (loops less than 100 nm in size).

Under normal LACBED conditions, the shadow image of a small loop is too small with respect to the diffraction pattern so that the splittings are not clearly visible (Figure 5a). The solution involves enlarging the shadow image by choosing a very small defocus value Δh, as shown on Figure 5b but in this case, it is required to use a very small selected-area aperture in order to separate the transmitted beam from the diffracted beam. A 2µm aperture is well suited to this purpose.

The second problem is that the contrast of the dislocation loop is strongly dependent on the diffraction conditions and these conditions change from one point to another on a LACBED pattern. ~~Away from a strong dynamical Bragg line or from an intersection with another Bragg line, we can consider that the two-beam conditions are locally verified~~. Loop contrast can be very strong at close proximity to a dynamical line (with s slightly positive) (see for example, Figures 6a and b) and vanishes as soon as the loop is away from this line (Figure 6c). This means that the dislocation loop can disappear when it is moved from one Bragg line to another in order to obtain a new splitting, and it becomes very difficult to avoid the risk of confusing the studied loop with other loops located in the vicinity. This difficulty is particularly important in the case of small and numerous loops. To solve this problem, the best method is to create a contamination spot close to the studied loop (Figure 7a) by focusing an incident beam with a very small spotsize (about 10 nm) on the specimen for a few minutes. This spot acts as a loop marker because its contrast does not depend on the diffraction condition and it remains clearly visible on LACBED patterns (Figure 7b).

For a dislocation line, the shadow image is either rotated by 180° if $\Delta h>0$ or not rotated if $\Delta h<0$. For a dislocation loop, a 180° rotation also occurs between the shadow image for $\Delta h>0$ and $\Delta h<0$ (Figure 8) but the polarity of the dislocation line around the loop as well as the direction of the loop normal N_{Loop} remain unchanged. This means that experiments can either be performed with the specimen located above or below the object plane, which makes the experiments easier.

In addition to the experimental conditions described above for a line dislocation, some specific conditions must be fulfilled for loops. The best splittings are observed when the loop is set perpendicular (as close as possible) with respect to the optical axis of the microscope. This condition is not very strict though a loop observed edge on is not useful. It is also required that at least one part of the loop be located in the middle of the thin foil. In the case

of small dislocation loops, there are usually many loops present in the specimen and it is not very difficult to find a one located in the middle of the thin foil because it will display good splittings.

Experimental conditions and specimens

The LACBED patterns were obtained with a CM30 Philips transmission electron microscope working at 300 kV. The nanoprobe mode was used with a convergence semi-angle of about 2° and a spot size of about 10 nm. All the experiments were performed at room temperature and the patterns were recorded with a CCD camera.

Three different specimens were used for this study.

1. Model austenitic steel formed from high purity iron, chromium and nickel (Fe-18% at. Cr-14% at Ni) and submitted to irradiation with 700 keV Kr^{++} ions at 600°C for 20 minutes. This specimen has been studied extensively by conventional TEM methods and contains mainly interstitial loops with {111} loop planes and with 1/3<111> Burgers vectors. Some perfect loops with ½<110> Burgers vectors are also present. This specimen was used as a reference to validate the present LACBED procedure to characterise the loops.

2. An Al-1.1Cu-0.2Mg (at.%) alloy quenched from solution treatment at 525°C and then given a thermal ageing treatment at 150°C for 60 seconds. It contains small loops having an average size of 50 nm.

3. A silicon cross-sectional specimen implanted with boron atoms. It contains small loops located a few microns under the surface.

The steel and the Al-Cu-Mg alloy were prepared by standard electropolishing techniques while the cross-sectional silicon specimen was prepared by mechanical polishing using the tripod method [13].

Description of the procedure used to characterise small loops

The full characterisation of a dislocation loop requires knowledge of the loop normal, $\mathbf{N_{Loop}}$, and the amplitude and sign of the Burgers vector **b**.

Identification of the loop normal $\boldsymbol{N_{Loop}}$

The loop normal $\mathbf{N_{Loop}}$ can be inferred from conventional TEM micrographs obtained from different [uvw] zone axes that give the projection of the studied loop. If several zone axes are taken into account, then the loop normal can be obtained without ambiguity. In the example given in Figure 9, the [0-11] loop normal is identified from various micrographs. If the tilt range of the microscope allows a specific zone axis [uvw] to be reached where the loop is set perpendicular to the optical axis of the microscope (and the largest loop projection is observed), then the loop normal $\mathbf{N_{Loop}}$ is directly identified as [uvw]. This is the case for the [0-11] zone axis in Figure 9.

Alternatively, LACBED patterns can also be used to identify the loop normal [4]. In this case the simplest situation is observed when the loop is set parallel to the optical axis. The identification of the loop normal is straightforward as shown by the example in Figure 10. In this case the sign of the defocus value Δh must be taken into account.

The loops analysed in the present study are relatively large edge loops and the identification of the loop plane is straightforward. This identification can be very difficult or even impossible with smaller loops having an appreciable shear component [1].

Identification of the Burgers vector

Any specimen orientation **B** is valid for this identification, but it is better to select an orientation where the loop is nearly perpendicular to the optical axis. In order to facilitate the indexation of the Bragg lines, it is also advised to be close to a known zone axis. Since a loop

is strongly contrasted and therefore clearly visible when it is located close to a strong dynamic Bragg line (except for if **g.b**=0), it is recommended to consider Bragg lines located within the vicinity of a strong dynamical line as can be seen in Figures 7 and 11.

The loop is moved to several Bragg lines, taking into account the conditions described in the previous sections, by tilting the specimen so as to obtain useful splittings. Since the experiments are quick and easy to perform, many splittings can be recorded to give confident results.

Some examples of splittings are shown in Figures 11 and 12. The four splittings in Figure 11 correspond to the loop displayed in Figure 9 from the Al-Cu-Mg alloy, and characterise a perfect dislocation with Burgers vector 1/2[0-11], having a [0-11] loop normal as previously demonstrated. Once the loop normal $\mathbf{N_{Loop}}$ and the Burgers vector **b** are known, the loop type is inferred. In this case it is a vacancy loop. Note that the splittings obtained on the 042 and 0-4-2 Bragg lines (i.e. on hkl and -h-k-l Bragg lines) are identical.

The splittings shown in Figure 12 correspond to the irradiated steel and to the implanted silicon specimens. They display a more complex aspect since they correspond to interstitial loops with a <111> loop normal surrounded by a Frank partial dislocation with Burgers vector 1/3<111>. A stacking fault with fault vector **R**=1/3<111> is located inside the loop and this stacking fault also produces a typical effect on the Bragg line each time the **g.R** dot product is not integral. The Bragg line separates into a main line and a secondary line [14]. This stacking fault effect is clearly visible in Figure 12 for the splittings with n=1/3, 4/3, 5/3, 7/8 and 8/3 i.e. for non-integral **g.b** values. On the other hand, there is no effect of the stacking fault when **g.b**=integer. These splittings are in accordance with the Tanaka simulations made for partial dislocation lines [5].

Even with the extra complication in the splitting caused by the stacking fault, the experiments remain easy to perform especially because no special orientation of the crystal is required and many splittings can be obtained within a small orientation domain.

Discussion

With respect to the conventional TEM methods, the LACBED method presents several advantages. There is nearly no contamination imparted to the specimen when performing LACBED. The patterns also have excellent quality and many splittings can be obtained quite quickly so that LACBED experiments can be completed in a short period of time.

Some difficulties may be encountered with bent or buckled specimens; the corresponding LACBED patterns are distorted and it may be difficult to index the Bragg lines. A high density of loops is also a difficulty. The solution is to perform the experiments in the thinnest areas of the specimen where the loops are more dispersed.

The diffraction patterns obtained for different zone axes must be indexed in a coherent way. To fulfil this condition either Kikuchi patterns or LACBED patterns were used (see for example figure 9). In this study, the hkl indices of the Bragg lines as well as the direction of the corresponding deviation parameter, s, were obtained from the software "Electron Diffraction" [15].

The smallest loops that were analysed using the procedure presented in this paper were about 30 nm. It is expected that this limit will extend to even smaller sizes by using a smaller selected-area aperture (1µm or 0.5µm).

Conclusion

Using the LACBED technique, three types of small vacancy or interstitial loops surrounded by perfect or partial dislocations have been analysed. This technique allows the full

characterisation of dislocation loops down to a size of about 30 nm provided a 2 µm selected-area aperture is used and a contamination point is introduced to act as a loop marker. Since the experiments are easy and fast to perform, many splittings can be obtained making the Burgers vector identification accurate and unambiguous. The proposed procedure was validated with a test austenitic steel specimen containing known {111} interstitial loops surrounded by Frank partial dislocations with 1/3<111> Burgers vector. The procedure was also applied to identify small {110} vacancy loops with perfect dislocations **b**=1/2<110> present in an Al-Cu-Mg alloy and {111} interstitial loops with **b**=1/3<111> formed by boron implantation of a silicon specimen.

Acknowledgements

The authors would like to acknowledge the support of the FAST (French-Australian Science and Technology) programme. They also thank P.H. Albarède for providing the silicon specimen and Y. Serruys who performed the irradiations in the Van de Graaff accelerator of the SRMP.

References

[1] M.L. Jenkins and M.A. Kirk, Characterisation of radiation damage by transmission electron microscopy, Institute of Physics Series in Microscopy in Materials Science (Series Editors, B Cantor and M.J. Goringe (2001)

[2] M.A. Kirk, R. S. Davidson, M.L. Jenkins and R.D. Twesten, Phil. Mag. 85, 497 (2005)

[3] D. Cherns and A.R Preston, Proc. ICEM-11, Kyoto, 721-722 (1986).

[4] J.P. Morniroli and F. Gaillot, Ultramicroscopy **83** 227-243 (2000).

[5] M. Tanaka, M. Terauchi and T. Kaneyama, *Convergent-Beam Electron Diffraction*. vol. II, JEOL, Tokyo. (1988)

[6] J.P. Morniroli, *LACBED. Application to crystal defects*. Monograph of the SFμ, Paris, (2004).

[7] J.P. Morniroli and P. Vermaut, Journal de Physique III, 3 2165-2168 (1993).

[8] P. Cordier, J.P. Morniroli and D. Cherns, Philosophical Magazine A, 72 5 1421-1430 (1995).

[9] C.E. Jäger, E. Spiecker, J.P. Morniroli, and W. Jäger, Journal Phys. Cond. Matter, **14** 12777-12782 (2002).

[10] M. Tanaka, R. Saito, K. Ueno and Y. Harada, Journal of Electron Microscopy, 29 408-412 (1980)

[11] I.K. JORDAN, C.J. ROSSOUW and R. VINCENT, Ultramicroscopy, 35 3-4 237-243 (1991).

[12] D. Cherns and J.P. Morniroli, Ultramicroscopy, 53 167-180 (1994)

[13] J.P. Benedict, R. Anderson, S.J. Klepeis and M. Chaker, Mater. Res. Soc. Symp. Proc., 199 189 (1990).

[14] J.P. Morniroli, Materials Chemistry and Physics, 81 2-3 209-213 (2003).

[15] J.P. Morniroli, "Electron Diffraction", Software to simulate CBED and LACBED patterns. Lille, (1998)

Figure captions

Figure 1

Schematic description of the LACBED technique. In this drawing, the specimen is located above the object plane ($\Delta h>0$) and only the ray paths for the electrons that are exactly in

Bragg conditions for a unique set of (hkl) lattice planes are given. For the sake of clarity, the transmitted beam is selected by means of an aperture located in the object plane. Actually, the selected-area aperture, which is located in the image plane, makes this selection.

Figure 2

Schematic description of the Cherns and Preston rules used to identify the sign of the **g.b**=n product.

Figure 3

Experimental conditions required to obtain useful splittings at the intersection of a Bragg line with a dislocation line.

a - For a tilted dislocation line present in the specimen, the best splitting is observed at t/2.

b - Effect of decreasing the defocus value Δh on the splitting aspect.

c - Effect of changing the sign of Δh on the splitting aspect. The specimen is above (Δh>0) or below (Δh<0) the object plane.

d - Effect on the splitting aspect of the angle between the Bragg line and the trace of the dislocation line.

Figure 4

Conventions used in the present study.

a - Respective arrangements of the incident beam, the normal to the specimen **B** and the normal to the loop $\mathbf{N}_{\mathbf{Loop}}$.

b - Description of a vacancy edge loop and corresponding Burgers circuit.

c - Description of an interstitial edge loop.

Figure 5

Effect of the defocus value, Δh, on the magnification of the shadow image of a dislocation loop. For the sake of clarity, the aperture is located in the object plane. Actually, it is located in the conjugate image plane where it has the same effect.

a - Effect of a large defocus value. The separation of the transmitted and diffracted beams is large but the magnification of the shadow image of the loop is small.

b - Effect of a small defocus value. The separation of the transmitted and diffracted beams is small and a very small aperture is required to select the transmitted beam. The magnification of the shadow image of the loop is large.

Figure 6

Examples of the change in contrast of the shadow image of a dislocation loop depending on the position of the loop in the LACBED pattern.

a, b - The contrast is very strong because the loop is close to a strong dynamical line.

c - The contrast is weak because the loop is away from a strong dynamical line.

Figure 7

Identification of a dislocation loop by means of a contamination spot.

a - A contamination spot is created close to the studied loop and acts as a loop marker.

b - The contrast of the contamination marker does not depends on the diffraction condition and remains clearly visible on the LACBED pattern.

Figure 8

Effect of the sign of the defocus value Δh on the polarity, **u'**, and on the loop normal, $\mathbf{N}_{\mathbf{loop}}$, of the shadow image of a dislocation.

a - When the specimen is above the object plane ($\Delta h>0$), the shadow image of the loop is rotated by a 180° angle with respect to the loop in the specimen. The line direction **u'** is anticlockwise as is the line direction **u** in the specimen.

b - When the specimen is below the object plane ($\Delta h>0$), the shadow image of the loop is not rotated with respect to the loop in the specimen. The line direction **u'** is also along the anticlockwise direction.

Figure 9

Micrographs of a dislocation loop present within the Al-Cu-Mg alloy taken at different zone axes. The loop is perpendicular to the incident beam for the [0-11] zone axis, which means that the loop normal is [0-11]. The micrographs are located on a LACBED map drawn with the software "Electron Diffraction" [13].

Figure 10

Identification of the loop normal, $\mathbf{N_{Loop}}$, from a LACBED pattern.

a - LACBED ray paths for a loop parallel to the optical axis and for a negative Δh defocus value.

b - LACBED pattern showing the shadow image of a loop seen edge-on. The [-1-10] loop normal is obtained from this pattern.

Figure 11

Identification of the Burgers vector of the dislocation loop shown in Figure 9.

a - The splittings observed for the 0-4-2, 042, 2-4-2 and 153 Bragg lines lead to the Burgers vector **b**=1/2 [0-11].

b - A vacancy loop is inferred from the micrographs in Figure 9 and from the LACBED patterns on Figure 11a.

Figure 12

Examples of experimental and schematised splittings obtained from the irradiated steel specimen and the boron implanted silicon specimen. They correspond to interstitial loops with <111> loop normal surrounded by a Frank partial dislocation with **b**=1/3<111>. Note the effect of the stacking fault with fault vector **R**=1/3<111> for the non-integral values of n.

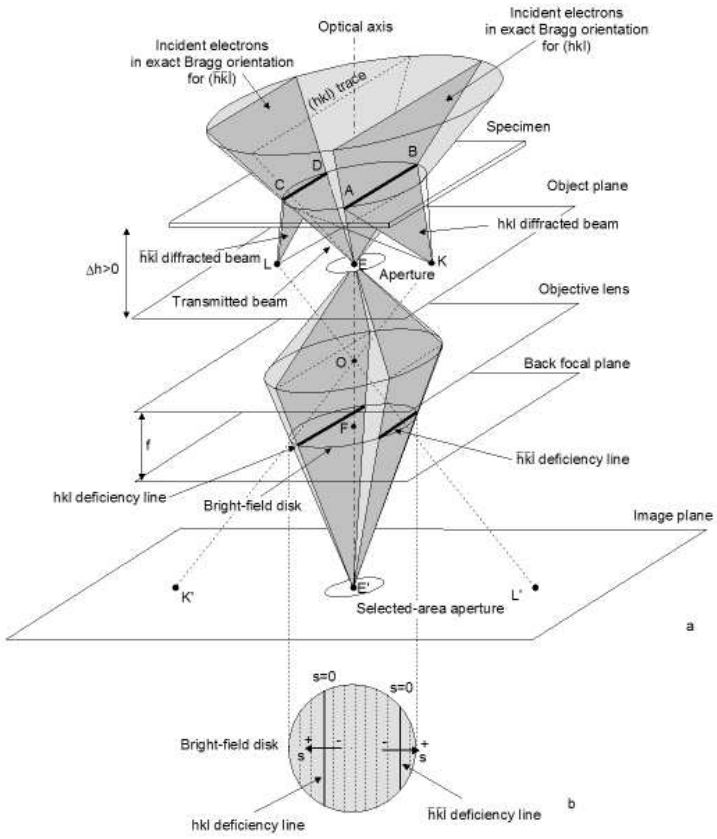

243x203mm (75 x 75 DPI)

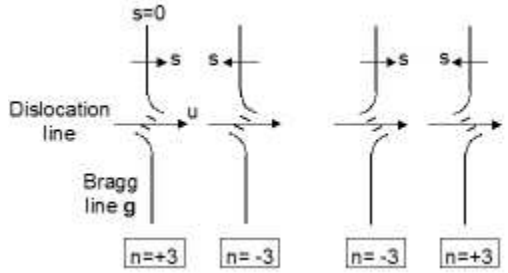

84x46mm (75 x 75 DPI)

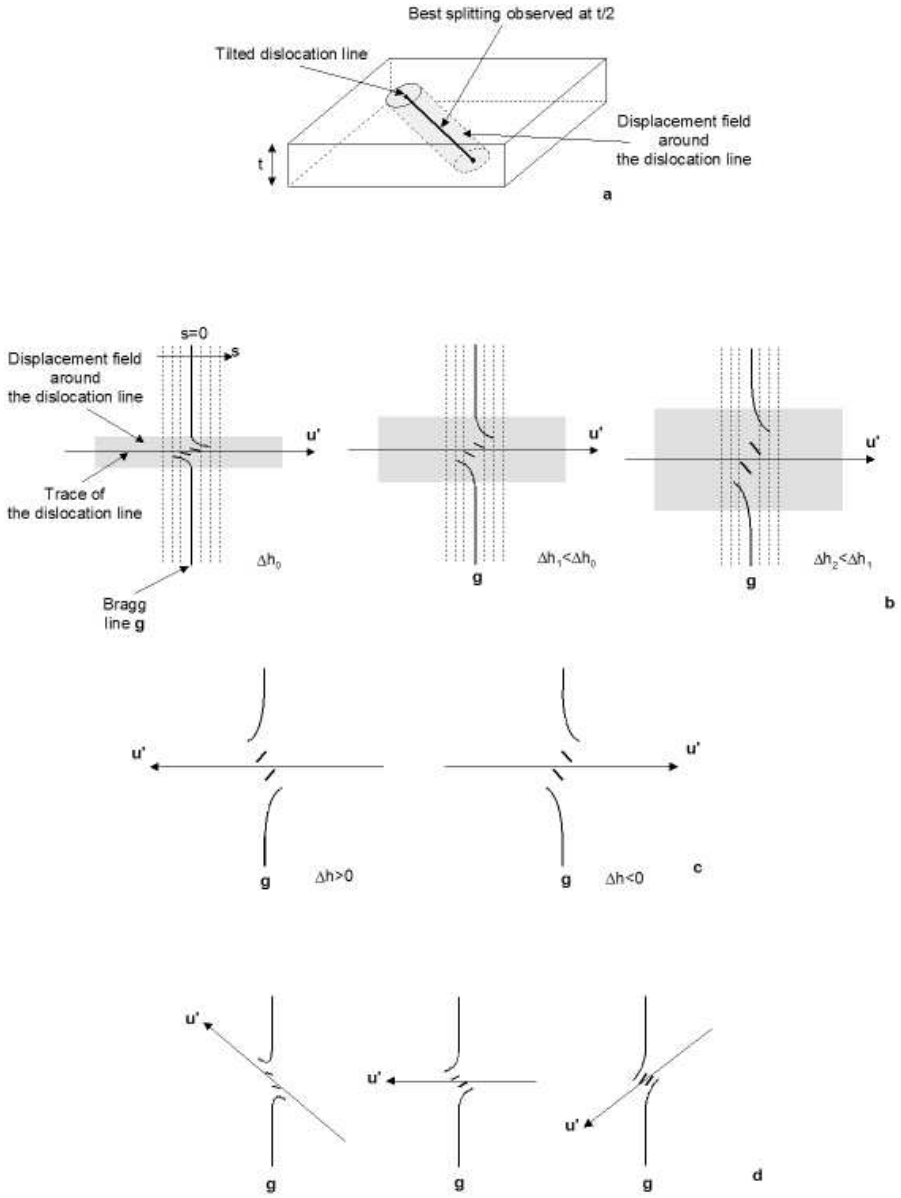

191x257mm (75 x 75 DPI)

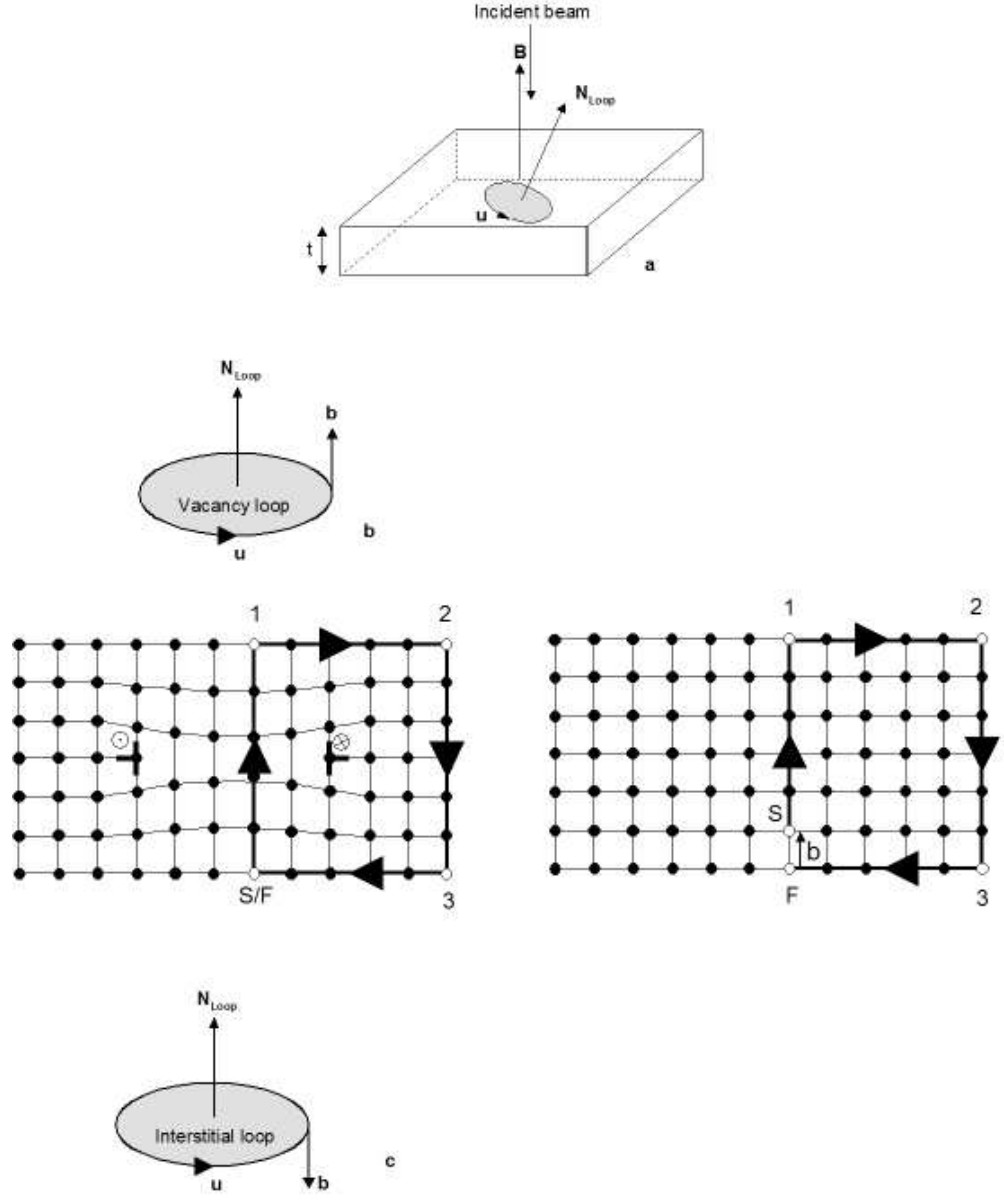

186x226mm (75 x 75 DPI)

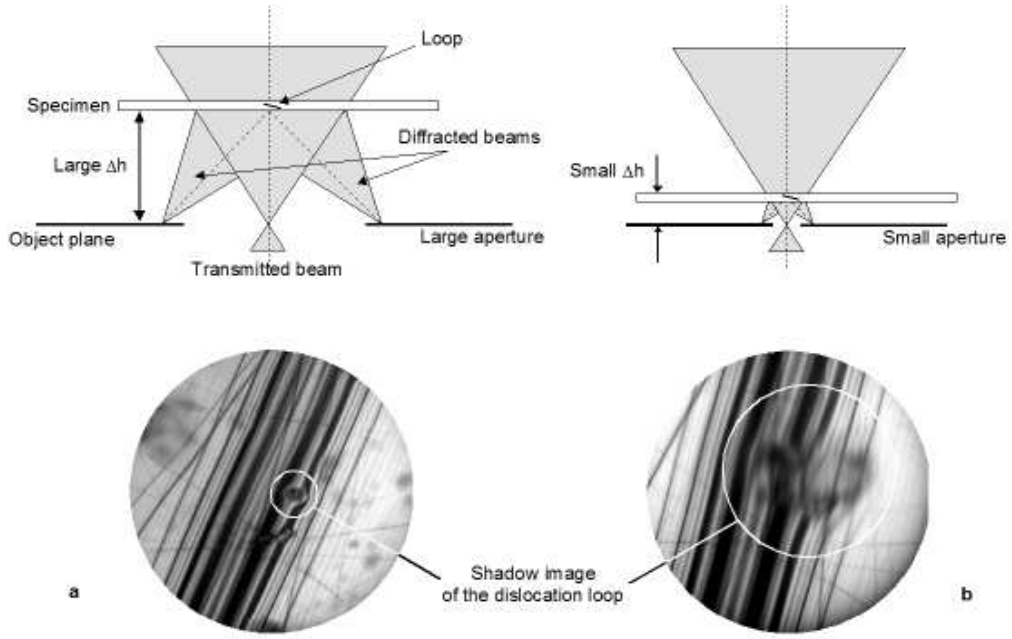

186x119mm (75 x 75 DPI)

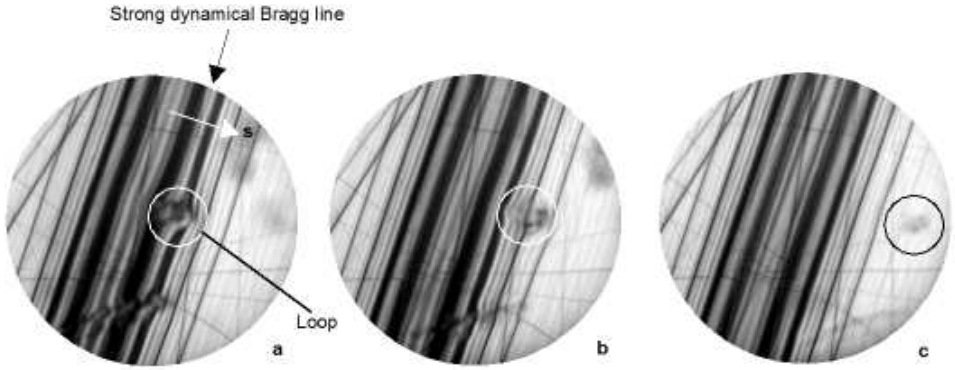

187x73mm (75 x 75 DPI)

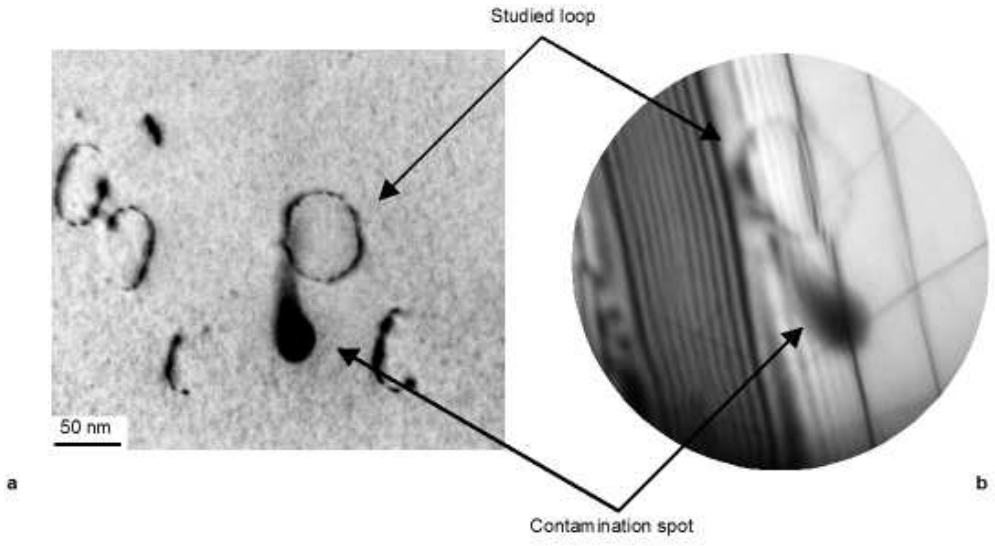

185x100mm (75 x 75 DPI)

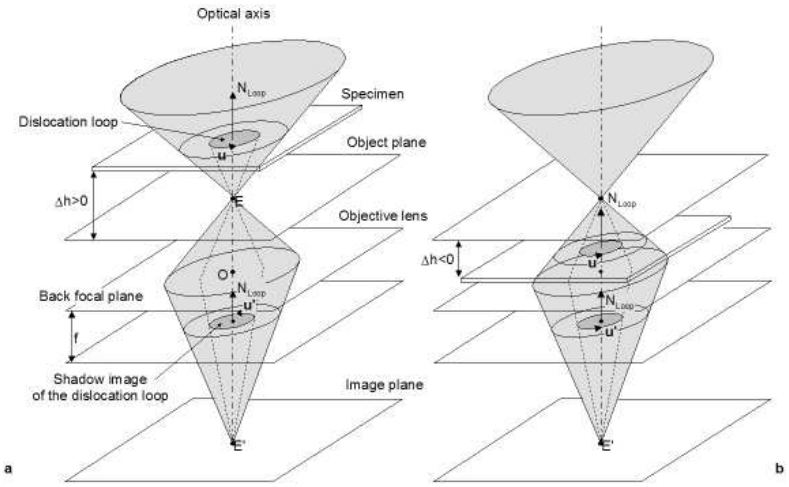

248x170mm (75 x 75 DPI)

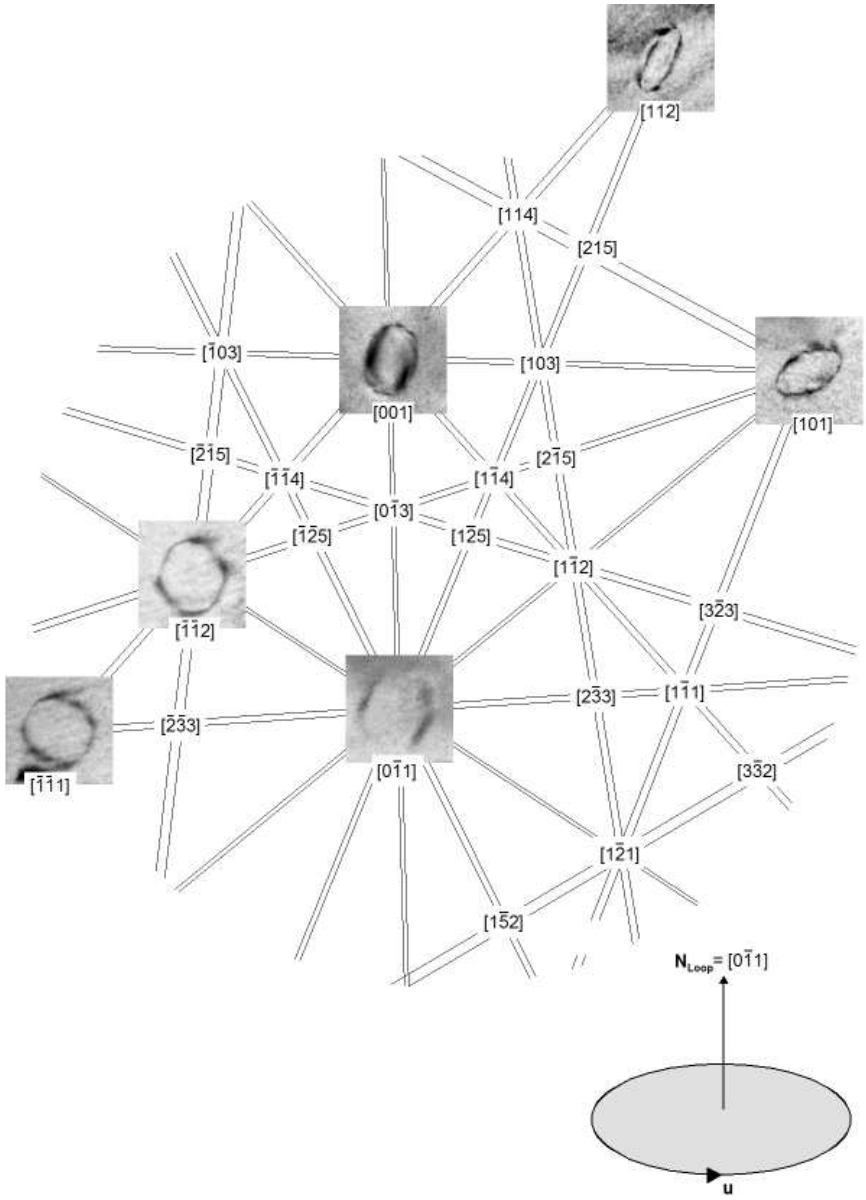

201x281mm (75 x 75 DPI)

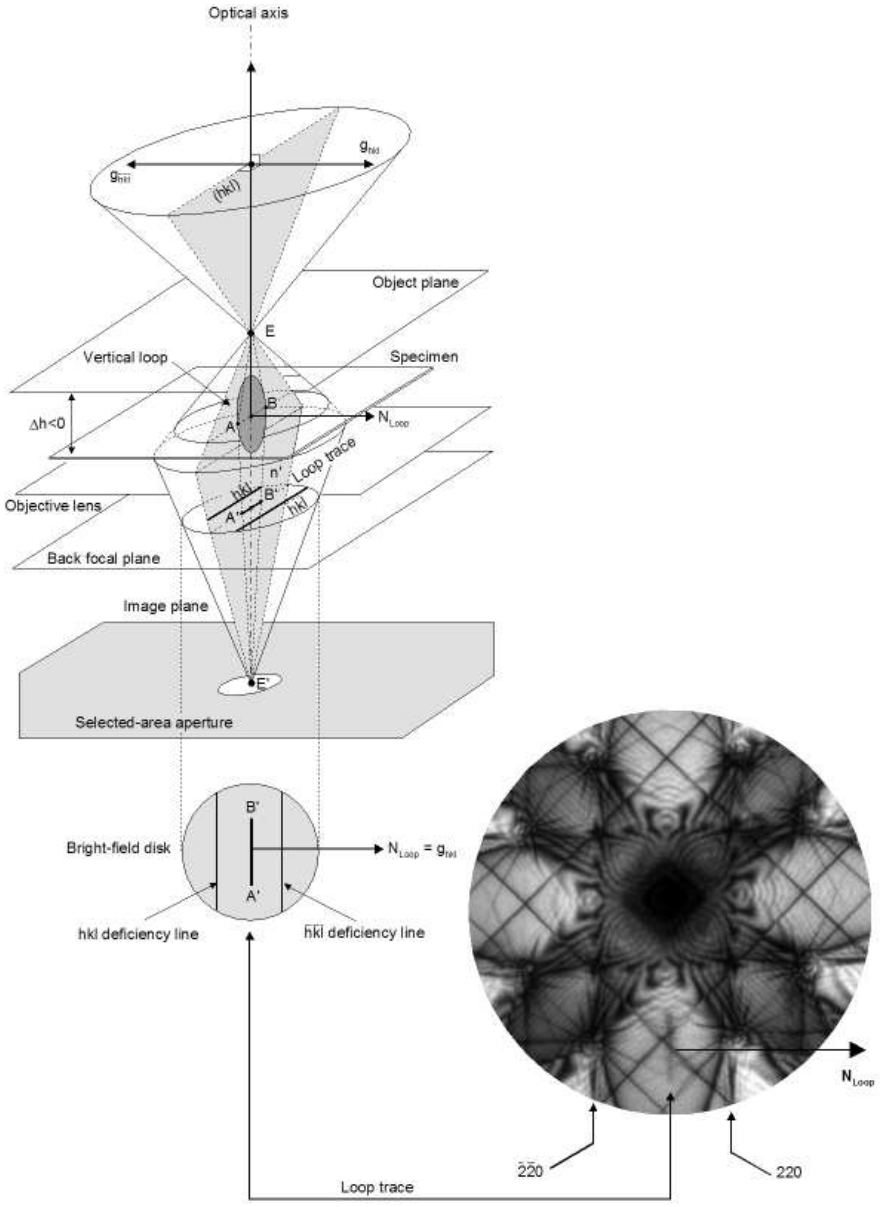

200x273mm (75 x 75 DPI)

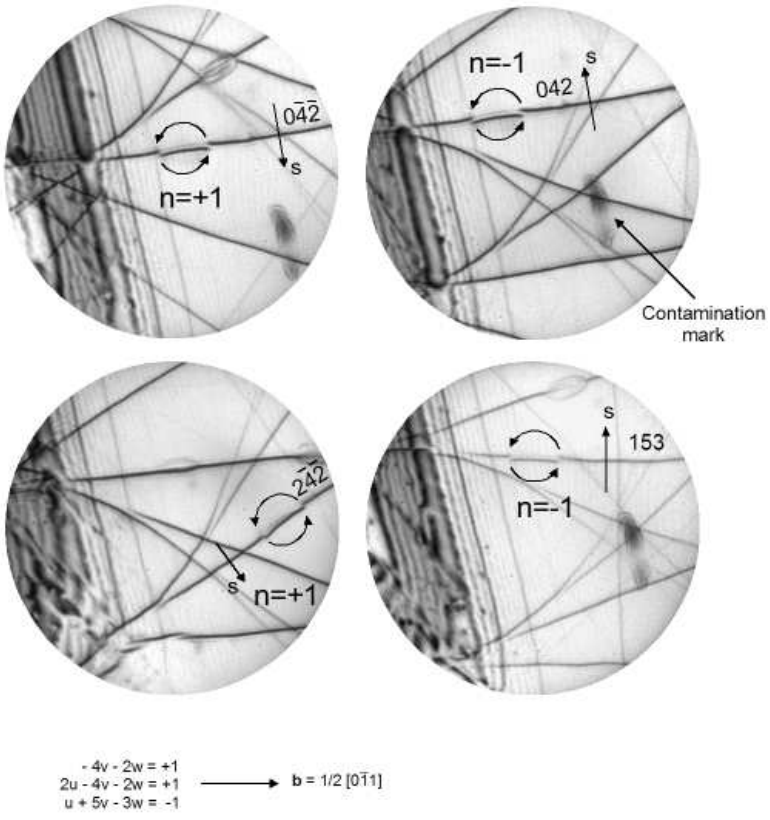

$$\begin{aligned} -4v - 2w &= +1 \\ 2u - 4v - 2w &= +1 \\ u + 5v - 3w &= -1 \end{aligned} \longrightarrow \mathbf{b} = 1/2\,[0\bar{1}1]$$

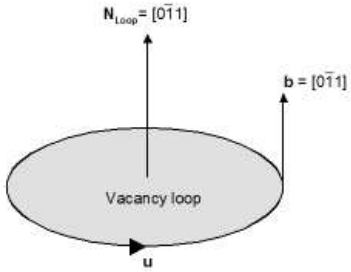

169x263mm (75 x 75 DPI)

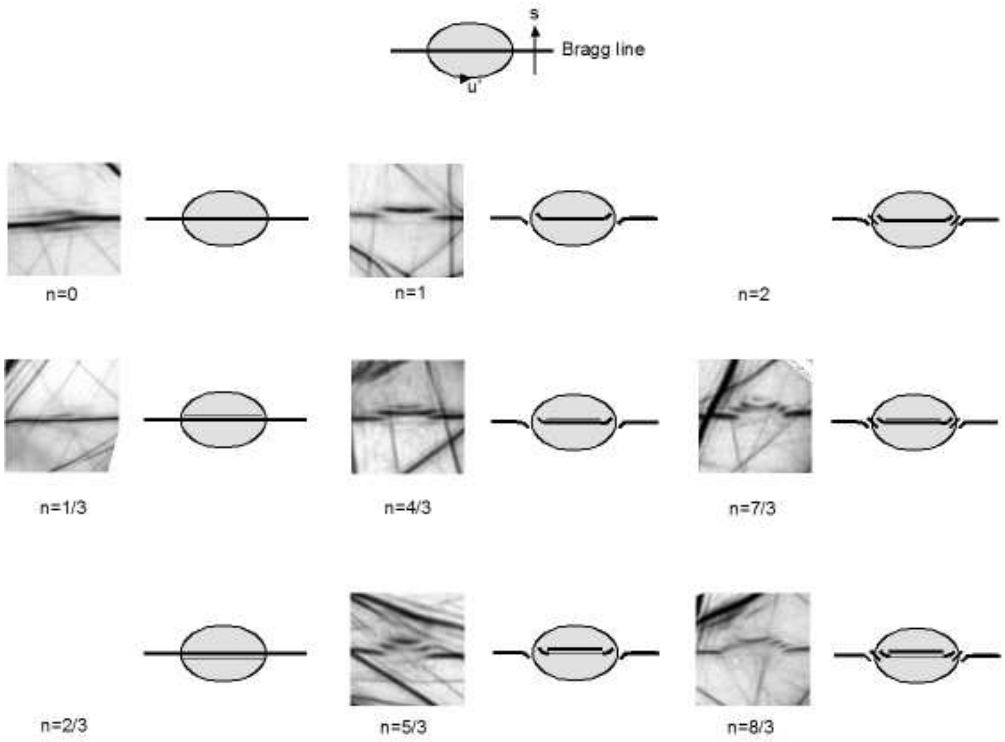

190x141mm (75 x 75 DPI)